

## Hyperfine tails and exchange-field distributions in amorphous magnetic spin glasses

M. E. Lines and M. Eibschutz

*AT&T Bell Laboratories, Murray Hill, New Jersey 07974*

(Received 8 April 1985)

Almost nothing is yet known about the nature of the "frozen disorder" of magnetic moments in concentrated magnetic spin glasses (or "speromagnets") such as (amorphous)  $a$ -YIG (yttrium iron garnet),  $a$ -FeF<sub>3</sub>, and  $a$ -NaFeF<sub>4</sub>, beyond the qualitative description of "randomlike." This paper probes the nature of the nearest-neighbor spin correlations in such systems by analysis of hyperfine-field distributions as measured by 4.2-K Mössbauer spectroscopy. Low-field tails are found to exist on the hyperfine distribution spectra of amorphous speromagnets but not amorphous ferromagnets. They indicate the presence of low-energy *exchange-field* states in the former caused by the cancellation of nearest-neighbor contributions within the frustrated spin network. Their interpretation has been used to determine the detailed exchange distribution function for  $a$ -YIG,  $a$ -FeF<sub>3</sub>, and  $a$ -NaFeF<sub>4</sub> and, by comparison of the results to the expectation for a set of randomly oriented spins, to monitor the nature of nearest-neighbor spin frustration in those amorphous speromagnetic systems.

### I. INTRODUCTION

All amorphous systems containing a high enough concentration of localized magnetic moments appear to undergo magnetic transitions as the temperature is lowered to phases in which each spin  $\mathbf{S}_i$  acquires a nonzero time-averaged value  $\langle \mathbf{S}_i \rangle$ . These "magnetically ordered" phases fall into one of two classes, according to whether they possess, or do not possess, a bulk magnetic moment. For the purpose of this paper these two classes are referred to as ferromagnetic and "speromagnetic,"<sup>1</sup> respectively, without any further implied restrictions. Experimentally, most amorphous ferromagnets are metallic, while amorphous speromagnets occur both in metals<sup>2</sup> and nonmetals.<sup>3</sup>

In the course of conducting <sup>57</sup>Fe Mössbauer experiments on several amorphous iron-containing ferromagnets and speromagnets we have observed<sup>4-6</sup> a feature of hyperfine-field distribution  $p_{\text{hf}}(H)$  at 4.2 K which is consistently present in speromagnets and absent in ferromagnets. It is an extended low-field tail on  $p_{\text{hf}}(H)$  which signifies the presence of a non-negligible fraction of spins which are not close to saturation  $|\langle \mathbf{S}_i \rangle| \approx S$  at 4.2 K, even when the spin-ordering temperature is an order of magnitude or more higher. These are spins which experience an exchange field  $H_{\text{ex}}$  for which  $g\mu_B H_{\text{ex}} \lesssim kT$  (with  $T=4.2$  K) and implies the presence of low-field states in the exchange-field distribution  $p_{\text{ex}}(H_{\text{ex}})$  as well. In general, speromagnetism results from magnetic frustration; the inability of spins to simultaneously minimize all pair exchange interactions  $2J_{ij}\mathbf{S}_i \cdot \mathbf{S}_j$  for topological reasons. The result is an outwardly randomlike orientational configuration of "frozen" spins. Most theoretical work<sup>7,8</sup> on the form of the function  $p_{\text{ex}}$  for systems of this kind has been performed in the context of the classic metallic "spin glasses" for which the concentration of magnetic atoms is small but the exchange interaction range  $r$  large. Conclusions here favor the existence of a "hole" in the exchange distribution at small fields. Thus, for example, in a Ruderman-Kittel-Kasuya-Yosida-like model,<sup>9</sup> with

$J_{ij} \propto r^{-3}$  and alternating in sign with increasing range, the computer generated  $p_{\text{ex}}$  shows a distribution which is only modestly perturbed<sup>8</sup> from the random-spin molecular-field approximation

$$p_{\text{ex}}(H_{\text{ex}}) \propto \eta H_{\text{ex}}^2 / (H_{\text{ex}}^2 + \eta^2), \quad (1)$$

where  $\eta$  is a constant proportional to the spin concentration.

In speromagnetic insulators, such as amorphous  $a$ -YIG (yttrium iron garnet),  $a$ -FeF<sub>3</sub>, and  $a$ -NaFeF<sub>4</sub>, exchange interactions  $J_{ij}$  are not only restricted to single-anion-bridged nearest neighbors (NN), but are dominantly (and in some cases probably exclusively) of one sign, viz. anti-ferromagnetic. In these cases frustration is presumably produced by the presence of odd-numbered rings of anti-ferromagnetically interacting spins although, to our knowledge, no modeling of the magnetism of such amorphous speromagnets has yet been carried out.

In this paper we calculate first the theoretical distribution  $p_{\text{ex}}$  of exchange fields for a *rigorously* randomly oriented molecular-field configuration of magnetic moments, each with  $z$  nearest neighbors (NN) magnetically interacting via a NN-only Heisenberg exchange coupling  $2J\mathbf{S}_i \cdot \mathbf{S}_j$ . This distribution is found to have no exchange hole as  $H_{\text{ex}} \rightarrow 0$  and, in fact, reaches its maximum value at  $H_{\text{ex}} = 0$ . Such a distribution has a significant number of tail states. However, via the intermediary of the hyperfine-field distribution as deduced from Mössbauer-Zeeman spectra, we are able to extract  $p_{\text{ex}}(H_{\text{ex}})$  for  $a$ -YIG,  $a$ -FeF<sub>3</sub>, and  $a$ -NaFeF<sub>4</sub> and find that, while all are qualitatively similar, they are *grossly* different from the random-spin orientation distribution. In particular, they all do possess an exchange hole as  $H_{\text{ex}} \rightarrow 0$  which must therefore be entirely produced by exchange-induced NN-spin correlations.

Section II calculates  $p_{\text{ex}}(H_{\text{ex}})$  in a random-orientational approximation. Section III presents the Mössbauer-Zeeman evidence for the existence of tail states in the amorphous ferric speromagnets and their absence in

amorphous ferromagnets. Section IV describes the manner in which the grosser aspects of hyperfine-field distribution (such as linewidth) in these speromagnets reflect the local magnetic coordination of the iron atoms while Sec. V sets out the manner in which the finer details of hyperfine line *shape* (including the tails) can be used to determine the actual exchange distribution. The experimentally determined  $p_{\text{ex}}(H_{\text{ex}})$  is contrasted with the random-orientational approximation of Sec. II in Sec. VI and a final summary is given in Sec. VII.

## II. THE RANDOM-SPIN-ORIENTATION MOLECULAR-FIELD APPROXIMATION

Consider the zero-temperature limit of an assembly of randomly oriented saturated spins  $S$  subject to the Hamiltonian

$$\mathcal{H} = \sum_i \sum_j J_{ij} \mathbf{S}_i \cdot \mathbf{S}_j. \quad (2)$$

If each spin  $\mathbf{S}_i$  is assumed to interact equally ( $J_{ij}=J$ ) with  $z$  nearest-neighbor spins, but not ( $J_{ij}=0$ ) with further neighbors, the exchange field experienced by a representative spin  $\mathbf{S}_0$  is

$$p_z(h) = \int_0^\pi d\theta_1 \sin\theta_1 \int_0^\pi \cdots \int_0^\pi d\theta_{z-1} \sin\theta_{z-1} \int_0^\pi \delta \left[ h - \sum_{n=1}^z \cos\theta_n \right] d\theta_z \sin\theta_z. \quad (4)$$

Writing  $x_n = \cos\theta_n$  for all  $n=1, 2, \dots, z$ , this simplifies to

$$p_z(h) = \int_{-1}^1 dx_1 \int_{-1}^1 \cdots \int_{-1}^1 dx_{z-1} \int_{-1}^1 dx_z \delta \left[ h - \sum_{n=1}^z x_n \right]. \quad (5)$$

For small coordination numbers  $z$  the integrals of Eq. (5) can be performed directly, but with increasing algebraic complexity as  $z$  increases. Analytic results for  $z=1, 2, 3, 4$  are given in Table I. For larger coordination numbers numerical results are easier to obtain via the integral representation of the  $\delta$  function by use of which the

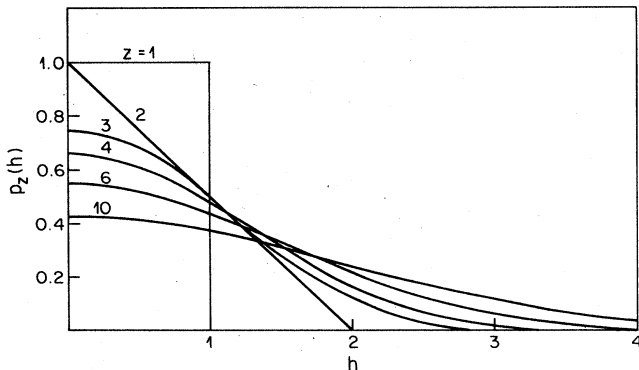


FIG. 1. Distribution  $p_z(h)$  of exchange fields  $H_{\text{ex}}=2JSh/g\mu_B$  evaluated from Eq. (6) for a randomly oriented distribution of  $z$  nearest-neighbor spins. Areas under the curves are normalized to unity.

TABLE I. The distribution  $p_z(h)$  of Eq. (5) for  $z=1, 2, 3, 4$ .

$z=1$	$p_1(h) = \begin{cases} 1, & 0 < h < 1 \\ 0, & h > 1. \end{cases}$
$z=2$	$p_2(h) = \begin{cases} 2-h, & 0 < h < 2 \\ 0, & h > 2 \end{cases}$
$z=3$	$p_3(h) = \begin{cases} 3-h^2, & 0 < h < 1 \\ (9-6h+h^2)/2, & 1 < h < 3 \\ 0, & h > 3 \end{cases}$
$z=4$	$p_4(h) = \begin{cases} (32-12h^2+3h^3)/6, & 0 < h < 2 \\ (64-48h+12h^2-h^3)/6, & 2 < h < 4 \\ 0, & h > 4 \end{cases}$

$$H_{\text{ex}} = (2JS/g\mu_B) \sum_{n=1}^z \cos\theta_n, \quad (3)$$

in which  $\cos\theta_n = \mathbf{S}_0 \cdot \mathbf{S}_n / S^2$  and  $\mu_B$  is the Bohr magneton. For randomly oriented NN spins it follows that the distribution of reduced fields  $h = g\mu_B H_{\text{ex}} / 2JS$  over all states is given by

multidimensional integral of Eq. (5) can be transformed to the one-dimensional form

$$p_z(h) = (1/\pi) \int_0^\infty [2(\sin K)/K]^z \cos(Kh) dK. \quad (6)$$

Using Eq. (6), numerical computations for the distribution functions  $p_z(h)$ , normalized to unit-total probability, have been obtained and are shown in Fig. 1 for coordination numbers up to  $z=10$ . In general they are seen to peak at zero field ( $h=0$ ) and, of course, for  $z \leq 4$  conform with the exact representations of Table I.

## III. HYPERFINE TAILS

In Fig. 2 we show the experimental  $^{57}\text{Fe}$  Mössbauer-Zeeman spectra for (a) the amorphous ferromagnetic metal<sup>10</sup>  $\text{Fe}_{82}\text{B}_{18}$  and (b) amorphous speromagnetic insulator<sup>4</sup>  $\alpha\text{-FeF}_3$ . Each is typical of its class; the former with very broad overlapping lines resulting primarily from local variations of magnetic moment with metalloidal environment in the unfilled  $d$ -band context of the metal, and the latter with much narrower quasisdiscrete lines in the fully localized  $3d^5$  context of the ferric ion.

More accurately, each Zeeman line on both types of spectrum has additional significant width contributions

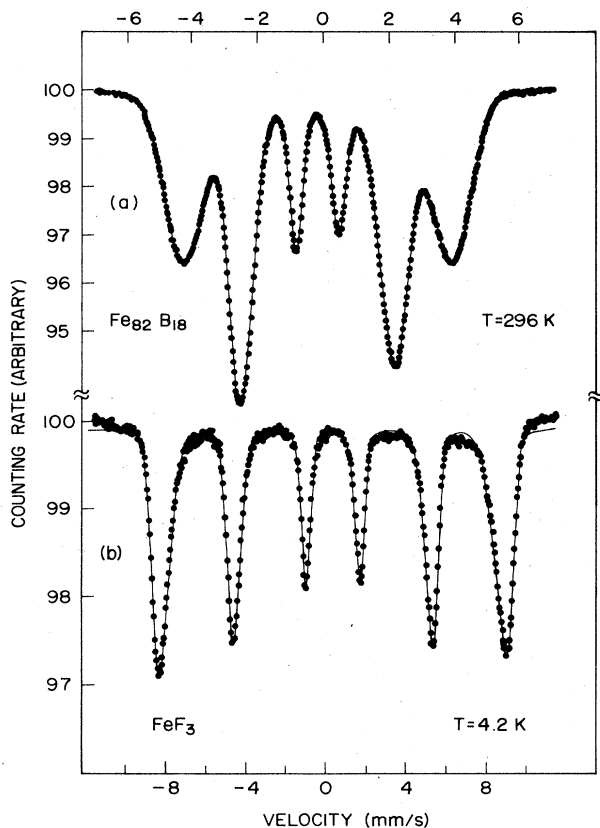


FIG. 2. (a) Mössbauer-Zeeman spectrum of ferromagnetic amorphous  $\text{Fe}_{82}\text{B}_{18}$  at  $T=296$  K. (b) Corresponding spectrum for speromagnetic amorphous  $\text{FeF}_3$  at  $T=4.2$  K.

from three sources—distributions of isomer shifts, electric field gradients, and hyperfine fields. Since each source contributes in a different way to each line, quantitative fits to the data are most readily obtained heuristically as the sum of independent distributions of natural-width Lorentzian lines. In an amorphous environment these distributions are commonly assumed to decay exponentially in the wings and, if such be the case, excellent trial fits can often be obtained<sup>4,5,10</sup> in terms of asymmetric Gaussians with remaining deviations studied by means of the computer-generated residuals.

Regardless of the details, if the distributions do decay rapidly in the wings then the fitting procedure, when iterated to convergence by means of a least-mean-squares subroutine, must accurately match the background at the extreme ends of the spectrum. If, on the other hand, an extended tail of nonexponential form should exist on the low-energy side of the distribution, then it will manifest itself in several ways, but most simply in a background mismatch. This we depict schematically in Figs. 3(a) and 3(b) for a single-line example with two types of low-energy tail, one which goes to zero as the energy goes to zero and one which does not.

We have analyzed the degree of background mismatch of converged computer Zeeman fits (using six independent asymmetric Gaussian distributions of natural-width

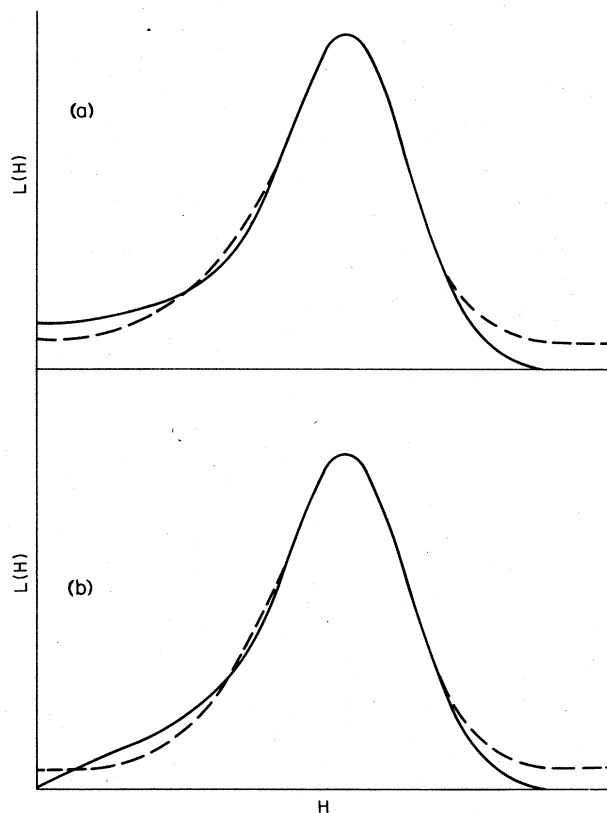


FIG. 3. Schematics of two hyperfine lineshapes  $L(H)$  which contain extended nonexponential “low-field” tails as  $H \rightarrow 0$  (solid curves) and the best (i.e., converged) least-squares fits obtainable using asymmetric Gaussian trial functions (dashed curves). Note the form of the misfits in the wings.

Lorentzian lines) for three amorphous metallic ferromagnets and three amorphous speromagnetic insulators. Using folded 1024-channel spectra,<sup>4,5,10,11</sup> the deviation of the fit from the data, averaged over the 25 channels at each extreme end of the spectra and expressed as a percentage of the outside line ( $L_1$  and  $L_6$ ) amplitude in each case, is (A) metallic ferromagnets ( $T=300$  K) (Refs. 6 and 10):

$$\begin{aligned} a\text{-Fe}_{82}\text{B}_{18} & (0.1 \pm 0.6)\% , \\ a\text{-Fe}_{75}\text{P}_{16}\text{B}_6\text{Al}_3 & (0.0 \pm 0.6)\% , \\ a\text{-Fe}_{83}\text{P}_{17} & (-0.3 \pm 1.5)\% ; \end{aligned} \quad (7)$$

and (B) insulator speromagnets ( $T=4.2$  K) (Refs. 4, 5, and 11):

$$\begin{aligned} a\text{-Y}_3\text{Fe}_5\text{O}_{12} & (0.6 \pm 0.4)\% , \\ a\text{-FeF}_3 & (4.0 \pm 0.9)\% , \\ a\text{-NaFeF}_4 & (4.7 \pm 3.9)\% . \end{aligned} \quad (8)$$

The error bars represent the root-mean-square (RMS) fluctuations of the experimental data and in no case is there a statistically significant difference between the two spectral ends.

A pattern emerges. The metallic ferromagnetic spectra, which with their very broad overlapping lines should be the more difficult to interpret using a simple heuristic model, have no statistically significant mismatch whereas the insulator speromagnets all have a mismatch which exceeds one standard deviation in the experimental scatter. The mismatch is most clearly evident for  $\alpha$ -FeF<sub>3</sub> and, in fact, is easily visible to the eye in Fig. 2(b).

Since the major lines (1, 2, 5, and 6) of the six-line Zeeman spectra are dominated by the distributions of hyperfine fields, we conclude that this mismatch, where it occurs, is produced by a low-field tail on the hyperfine distribution  $p_{\text{hf}}(H)$ . The latter must be due to the existence of some iron sites for which the thermally averaged electronic spin is very markedly reduced from saturation. This, in turn, implies the existence of some iron sites for which the exchange field energy  $g\mu_B H_{\text{ex}} \leq kT$ . We conclude that such sites do not exist in the amorphous metallic ferromagnets which we have studied (even at room temperature) while they do exist in each of the insulator speromagnets even at 4.2 K. Physically one would anticipate that these abnormally low exchange-field sites arise in speromagnets as the result of the exchange cancellations produced by the complex orientational configurations of NN spins. In particular, they obviously do exist in the random orientational approximation of Fig. 1.

#### IV. LOCAL STRUCTURES

The hyperfine field  $\mathbf{H}$  for ferric nuclei has two principal components  $\mathbf{H}_{\text{loc}}$  and  $\mathbf{H}_{\text{ST}}$ .<sup>12,13</sup> The local component

$$\mathbf{H}_{\text{loc}} = -CS_0/S \quad (9)$$

is proportional to the electronic spin  $S_0$  on the site in question, while the supertransferred component

$$\mathbf{H}_{\text{ST}} = \sum_n B_n \mathbf{S}_n / S \quad (10)$$

has contributions from all single-bridged nearest-neighbor iron spins  $\mathbf{S}_n$ . In particular, for ferric ions the supertransferred coefficients  $B_n$  depend on iron-anion-iron bond angles  $\phi_n$  in a known fashion,<sup>12,13</sup> viz.

$$B_n = H_\pi + (H_\sigma - H_\pi)\cos^2\phi_n, \quad (11)$$

where  $H_\pi$  and  $H_\sigma$  are known for many materials. For example, their values (in kOe) for YIG, FeF<sub>3</sub>, and NaFeF<sub>4</sub> are, respectively,<sup>5,14</sup>  $(H_\sigma; H_\pi) = (35; 6)$ ,  $(19; 3.5)$ , and  $(17.8; 3.2)$ .

Hyperfine linewidths  $\sigma(H)$  in ferric speromagnets are expected<sup>14</sup> to be dominated by their supertransferred component  $\sigma(H_{\text{ST}})$  as  $T \rightarrow 0$ . In  $\alpha$ -YIG and  $\alpha$ -NaFeF<sub>4</sub> we have earlier observed<sup>5,14</sup> that the use of Eq. (11) coupled with the assumption of quasirandom spin orientations adequately accounts for the experimental observations. For example, assuming a quasirandom spin-configurational ordering of  $\mathbf{S}_n$ , the mean-square fluctuation in the projection of  $\mathbf{H}_{\text{ST}}$  on  $\mathbf{H}_{\text{loc}}$  follows as<sup>14</sup>

$$\sigma^2(H_{\text{ST}}) = (z/3)(H_\sigma - H_\pi)^2(t^2 + 2t/3 + 1/5), \quad (12)$$

if  $\phi_n$  exhibits a random-packing distribution [where  $z$  is

the mean number of singly bridged magnetic NN and  $t = H_\pi / (H_\sigma - H_\pi)$ ], and as

$$\sigma^2(H_{\text{ST}}) = (z/3)[H_\pi + (H_\sigma - H_\pi)\cos^2\phi]^2, \quad (13)$$

if  $\phi_n \approx \phi$  is approximately constant, as expected for a quasicrystalline local structure.

Amorphous YIG is already known to be an essentially random-packed structure<sup>11,14</sup> with mean coordination number  $z \approx 5$ . From Eq. (12) we find that  $\sigma(H_{\text{ST}})$  accounts for 23 kOe of the measured total hyperfine width  $\sigma(H) = 29$  kOe at 4.2 K. The difference is presumably accounted for by  $C$  parameter variations in Eq. (9) due to the not insignificant distribution of local ligand coordinations in the random-packed environment.

Amorphous NaFeF<sub>4</sub> on the other hand, is known<sup>5</sup> to be quasicrystalline on a local scale with  $z = 4$ . Using Eq. (13) with  $\phi$  set equal to its crystalline value of 150° we find that  $\sigma(H_{\text{ST}})$  is 16 kOe. This compares with a measured  $\sigma(H)$  of 25 kOe at 4.2 K seemingly at odds with expectations, but the origin of the discrepancy is known.<sup>5</sup> It results from the fact that 4.2 K for this case alone is not a good approximation to  $T = 0$  since the spin ordering temperature for  $\alpha$ -NaFeF<sub>4</sub> is only 12 K (as opposed to 30 K for  $\alpha$ -FeF<sub>3</sub> and  $\sim 40$  K for  $\alpha$ -YIG). The extra contribution is due to a distribution of  $H_{\text{loc}}$  resulting from non-negligible thermal variations of local spin  $S_0$  in Eq. (9) for all (not just tail) spins in this case.

For  $\alpha$ -FeF<sub>3</sub> the random-packed or quasicrystalline nature of the local environment has not yet been determined and models of each type have appeared in the literature.<sup>15,16</sup> The determination can now be made using Eqs. (12) and (13). In the random-packed model of Ref. 15 the average magnetic coordination number is only  $z \approx 4$ , leading to a value  $\sigma(H_{\text{ST}}) = 11$  kOe from Eq. (12). Even if we raised this coordination to  $z = 6$  the supertransferred width is increased only to 14 kOe. The quasicrystalline result, using Eq. (13) with  $z = 6$  and  $\phi$  set equal to its crystalline value of 153°, provides a very different value,  $\sigma(H_{\text{ST}}) = 22$  kOe. Since the measured total hyperfine linewidth at 4.2 K is  $\sigma(H) = 24$  kOe, and there are no significant thermal perturbations of  $S_0$  for most spins in this case, the conclusion is clear:  $\alpha$ -FeF<sub>3</sub> is a quasicrystalline structure with predominantly sixfold magnetic coordination and should be modeled along the lines of Ref. 16.

Finally, from this section, we note for use below the following values deduced for RMS supertransferred hyperfine linewidths as  $T \rightarrow 0$ :

$$\begin{aligned} \sigma(H_{\text{ST}}) &= 23 \text{ kOe, } \alpha\text{-YIG} \\ \sigma(H_{\text{ST}}) &= 22 \text{ kOe, } \alpha\text{-FeF}_3 \\ \sigma(H_{\text{ST}}) &= 16 \text{ kOe, } \alpha\text{-NaFeF}_4. \end{aligned} \quad (14)$$

#### V. EXPERIMENTAL DETERMINATION OF EXCHANGE-FIELD DISTRIBUTIONS

The manner in which the distribution of exchange fields influences the hyperfine distribution at  $T = 0$  in ferric speromagnets has been set out in Ref. 14. It arises via the supertransferred hyperfine component  $H_{\text{ST}}$  since both

$H_{\text{ex}}$  and  $H_{\text{ST}}$  depend on the same Fe-anion-Fe local bridge angles in a closely-related manner. Assuming that a relationship between  $H_{\text{ex}}$  and  $H_{\text{ST}}$  can be expressed at least approximately in a functional manner

$$H_{\text{ex}} \sim f(H_{\text{ST}}), \quad (15)$$

then the form of the function  $f$  can be probed from the experimental hyperfine distribution  $p_{\text{hf}}(H_{\text{ST}})$  which can be determined from the shape of the outside Mössbauer-Zeeman lines  $L_1$  and  $L_6$  via their residuals. We examine in particular the computer-generated deviation of  $p_{\text{hf}}(H_{\text{ST}})$  from an equal area symmetric Gaussian,  $\exp(-H_{\text{ST}}^2/w_0^2)$ , the latter being assumed to adequately approximate the distribution when  $H_{\text{ex}}=0$ ,<sup>14</sup> i.e., to represent curves of the type  $p_z$  of Fig. 1 when  $z > 4$  (see also Fig. 14).

A trial function of the qualitatively anticipated form,<sup>14</sup> viz.

$$f(H_{\text{ST}}) \sim \exp(-\alpha^2 H_{\text{ST}}^2/w_0^2), \quad (16)$$

in terms of which the hyperfine shape deviation from  $\exp(-H_{\text{ST}}^2/w_0^2)$  takes the form [Eq. (5.17) and Fig. 4 of Ref. 14]

$$r(h) \sim h e^{-h^2} [e^{-\alpha^2 h^2} - (1 + \alpha^2)^{-1}], \quad (17)$$

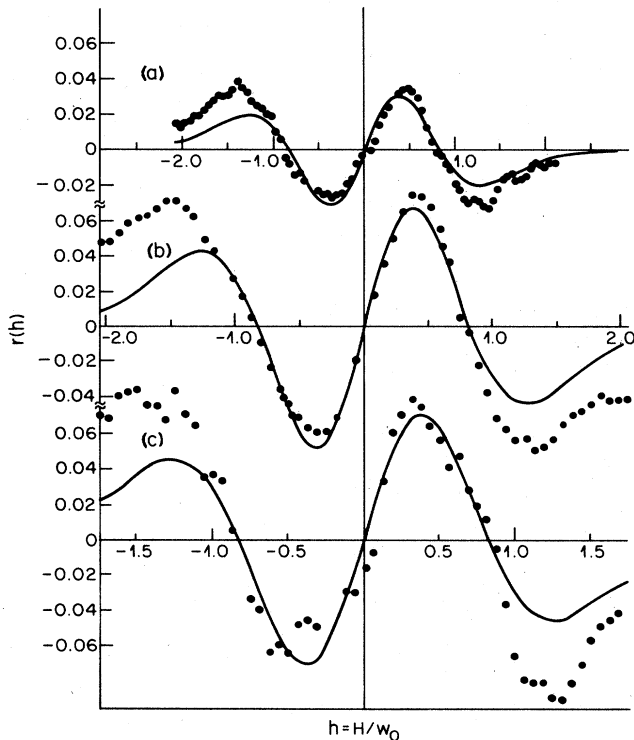


FIG. 4. Measured  $T=4.2$  K residuals  $r(h)$  of hyperfine line shape (solid circles) are compared with the theoretical forms (solid curves) of Eq. (17) with  $\alpha=1$  for (a)  $a$ -YIG, (b)  $a$ -FeF<sub>3</sub>, and (c)  $a$ -NaFeF<sub>4</sub>. The ordinate scale is given as a fraction of the parent symmetric-Gaussian peak value for each case and the abscissa is measured from this peak position as origin (i.e.,  $h=0$ ). Note that the abscissa scales are different for (a), (b), and (c).

where  $h = H_{\text{ST}}/w_0$  provides a convincing fit to the experimental data if  $\alpha = 1.0 \pm 0.3$  as shown in Figs. 4(a), 4(b), and 4(c) for  $a$ -YIG,  $a$ -FeF<sub>3</sub>, and  $a$ -NaFeF<sub>4</sub>, respectively, except in the wings. The discrepancies in the wings are merely another manifestation of the tail effect due to the finite temperatures (4.2 K) of measurement and will be elaborated below. Meanwhile, writing  $H_{\text{ex}} = a \exp(-\alpha^2 h^2)$  from Eqs. (15) and (16) and, in lowest order,  $p_{\text{hf}}(h) \sim \exp(-h^2)$ , we formally derive the corresponding unnormalized exchange distribution

$$p_{\text{ex}}(H_{\text{ex}}) = (H_{\text{ex}}/a)^{(1-\alpha^2)/\alpha^2} [\ln(a/H_{\text{ex}})]^{-1/2}, \quad (18)$$

which is shown in Fig. 5 for  $\alpha=0.8, 1.0$ , and  $1.2$ .

Since Eq. (16) is only a trial function of a qualitatively anticipated form, no great significance should be attached to the detailed algebraic form of Eq. (18). On the other hand, its qualitative shape is presumably realistic. The distribution  $p_{\text{ex}}(x)$  is zero or nonzero in the limit  $x \rightarrow 0$  according to whether  $\alpha \leq 1$  or  $\alpha > 1$  and rises to a maximum at  $x=1$  before dropping sharply to zero (Fig. 5). The divergencies at  $x=1$  for all  $\alpha$ , and as  $x \rightarrow 0$  when  $\alpha > 1$ , contained in the specific analytic form of Eq. (18), should probably be rounded to finite values in a less idealized approximation.

Defining tail states to be those for which  $g\mu_B H_{\text{ex}} \leq kT$ , the hyperfine tail amplitude near  $g\mu_B H_{\text{ex}} = kT$  (or equivalently for ferric ions  $\bar{S}/S \approx 0.77$ ) can be approximately measured as the summed deviation of theory and experiment in the wings of Fig. 4; viz.  $\sim 1.5\%$ ,  $\sim 5\%$ , and  $\sim 8\%$  of peak distribution for  $a$ -YIG,  $a$ -FeF<sub>3</sub>, and  $a$ -NaFeF<sub>4</sub>, respectively, at 4.2 K. The total fraction  $f$  of iron sites in this tail can be derived from these numbers only if the shape of the hyperfine tail is known. This, in turn, depends on the shape of the exchange distribution

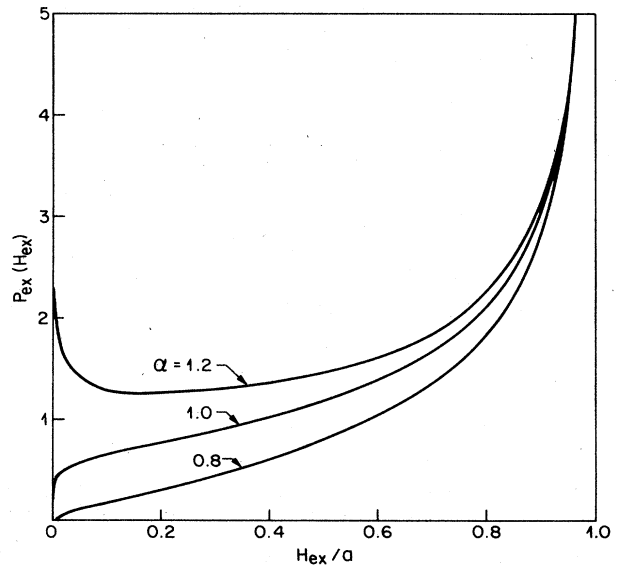


FIG. 5. Unnormalized exchange-distribution function  $p_{\text{ex}}(H_{\text{ex}})$  of Eq. (18) for the  $\alpha$  values 0.8, 1.0, and 1.2. The area under each curve (and hence the normalizing factor for the distribution) is  $\alpha\sqrt{\pi}$ .

TABLE II. Parameters relating to the exchange-field distribution of Eq. (18), or equivalently Eq. (6.8) of Ref. 14, as determined from residual fits to the theoretical form of Eq. (17) [or Eq. (5.13) of Ref. 14] for the trial  $\alpha$  values 0.8, 1.0, and 1.2. The detailed fits for  $\alpha=1.0$  are those shown in Fig. 4.

Material	<i>a</i> -YIG			<i>a</i> -FeF <sub>3</sub>			<i>a</i> -NaFeF <sub>4</sub>		
$w_0$ (kOe)	33			31			23		
$A^a$	0.014			0.028			0.033		
Trial $\alpha$ value	0.8	1.0	1.2	0.8	1.0	1.2	0.8	1.0	1.2
$c^a$ (kOe)	5.0	4.1	3.7	10.5	8.8	7.9	8.1	6.7	6.0
$a=c/A$ (kOe)	360	290	260	380	310	280	250	200	180
$H_{ex}^{max}$ (K)	48	39	35	51	42	38	33	27	24
$\langle H_{ex} \rangle$ (K)	38	28	22	40	30	24	26	19	15
% spins in the tail at 4.2 K	1	3	9	1	3	8	2	5	12

<sup>a</sup>Notation of Ref. 14.

$p_{ex}(H_{ex})$  in the region  $g\mu_B H_{ex} \leq kT$ . For  $p_{ex} = \text{const}$  in this region the explicit form for this tail has been given for ferric spins (Fig. 4 of Ref. 4) and, for this case, the above amplitudes translate into  $f$  values of  $\sim 2\%$ ,  $\sim 7\%$ , and  $\sim 11\%$ , respectively, at 4.2 K.

These  $f$  values may also be probed directly via a mean Zeeman line position analysis as set out in Ref. 4 since mean line positions depend on tail shape. Using the  $p_{ex} = \text{const}$  hyperfine tail shape, this latter analysis gives corresponding estimates of  $\sim 0\%$ ,  $\sim 3\%$ , and  $\sim 10\%$ . The inference is that while the  $p_{ex} = \text{const}$  approximation is self-consistent for *a*-NaFeF<sub>4</sub>, the other speromagnets have fewer states at low exchange fields than the  $p_{ex}(H_{ex}) = \text{const}$  distribution would require. Within the  $\alpha = 1.0 \pm 0.3$  band of values which provide acceptable residuals in Fig. 4, this suggests  $\alpha \approx 1.2$  for *a*-NaFeF<sub>4</sub> [for which value  $p_{ex}$  is flat over an extended range (see Fig. 5), and nonzero as  $H_{ex} \rightarrow 0$ ], while  $0.7 < \alpha < 1.0$  is the more relevant range for *a*-YIG and *a*-FeF<sub>3</sub> (with  $f \approx 1\%$  and  $4\%$ , respectively). Accordingly, a hyperfine tail shape of qualitative form as in Fig. 3(a) is indicated for *a*-NaFeF<sub>4</sub> and of form of Fig. 3(b) for the others. This difference is confirmed by examining the computer mismatch at the Zeeman spectra center ( $H = 0$ ) (between lines  $L_3$  and  $L_4$ ) where, averaging over the 11 center channels, we find mismatches:

$$\begin{aligned}
 & a\text{-YIG } (+0.1 \pm 0.8)\% , \\
 & a\text{-FeF}_3 (+0.1 \pm 0.7)\% , \\
 & a\text{-NaFeF}_4 (-2.6 \pm 2.6)\% ,
 \end{aligned} \tag{19}$$

statistically nonzero only for *a*-NaFeF<sub>4</sub> for which the sign is opposite to that of the equivalent "Zeeman-extreme" finding of Eq. (8) as expected from Fig. 3(a).

A final independent confirmation and refinement of these  $\alpha$  assignments may be obtained quite independently from the fit of the residual amplitudes in Fig. 4 as detailed in Ref. 14. Using the Gaussian relation  $w_0 = \sqrt{2}\sigma(H_{ST})$ , with  $\sigma(H_{ST})$  taken from Eq. (14) for each speromagnet, these amplitude fits (for any trial  $\alpha$  value) determine the maximum exchange energy  $H_{ex}^{max}$  [i.e., the parameter  $a$  in Eq. (18), or  $c/A$  in the notation of Ref. 14] and hence the complete exchange distribution

function  $p_{ex}(H_{ex})$ . Once this function is known for each trial  $\alpha$  value, the fraction  $f$  of sites for which  $g\mu_B H_{ex} \leq kT$  at any temperature is easily determined, as well as the mean exchange energy  $\langle H_{ex} \rangle$ . Quantitative results for *a*-YIG, *a*-FeF<sub>3</sub>, and *a*-NaFeF<sub>4</sub> for each of the trial values  $\alpha = 0.8, 1.0, \text{ and } 1.2$  are given in Table II. They conform with the known 4.2-K tail fractions if  $\alpha \approx 0.8$  (YIG),  $\approx 1.0$  (FeF<sub>3</sub>), and  $\approx 1.2$ , (NaFeF<sub>4</sub>). The resulting equally normalized exchange distributions are shown in Fig. 6.

Of particular interest is the mean exchange field  $\langle H_{ex} \rangle$  (in Kelvin units) experienced by the ferric spins in each speromagnet. Using Table II one observes a striking correlation between  $\langle H_{ex} \rangle$  and the corresponding spin-glass temperatures  $T_F$  as follows:

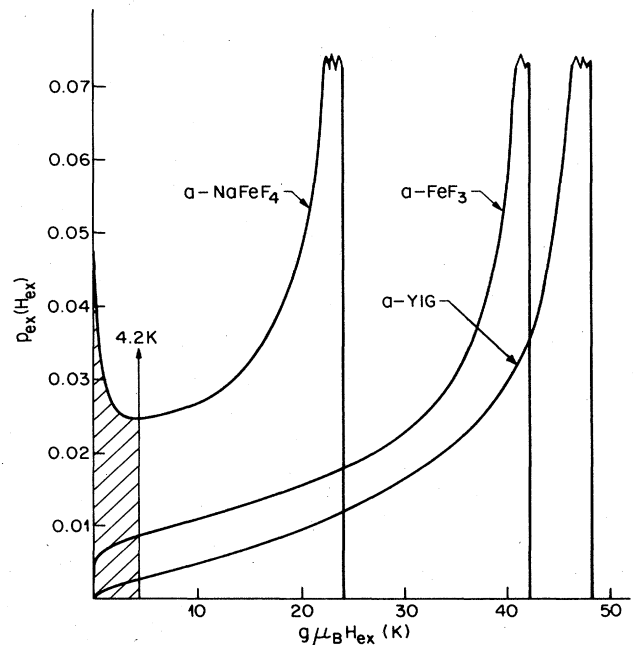


FIG. 6. Normalized exchange distributions  $p_{ex}(H_{ex})$  for the three ferric speromagnets *a*-YIG, *a*-FeF<sub>3</sub>, and *a*-NaFeF<sub>4</sub>. The "tail-states" at  $T=4.2$  K are shaded.

- $a$ -YIG,  $\langle H_{ex} \rangle \approx 38$  K,  $T_F \approx 40$  K (Ref.17),  
 $a$ -FeF<sub>3</sub>,  $\langle H_{ex} \rangle \approx 30$  K,  $T_F \approx 29$  K (Ref.18), (20)  
 $a$ -NaFeF<sub>4</sub>,  $\langle H_{ex} \rangle \approx 15$  K,  $T_F \approx 12$  K (Ref.18).

The suggestion is that

$$g\mu_B \langle H_{ex} \rangle_{T=0} \approx kT_F \quad (21)$$

for these  $S = \frac{5}{2}$  speromagnets, in approximate accord with the molecular-field expectation for ordering temperatures  $T_c$  in ferro- and antiferromagnets, viz.

$$kT_c = g\mu_B \langle H_{ex} \rangle_{T=0} (S + 1)/3. \quad (22)$$

## VI. THE SPEROMAGNETIC SPIN CONFIGURATION

Within a distorted crystalline model of  $a$ -FeF<sub>3</sub> and  $a$ -NaFeF<sub>4</sub> we expect distributions of exchange parameters  $J$  to be centered on their respective crystalline values of 14.5 K (Ref. 15) and 11.5 K (Ref. 19). The situation in  $a$ -YIG is more complex. However, within the random-packing model of Ref. 20 (in particular Fig. 12 of that paper) one can calculate the major (kinetic) component of  $\langle J \rangle$  from its known dependence on bond angle<sup>13</sup>

$$J = cH_\sigma [2H_\pi + (H_\sigma - 2H_\pi)\cos^2\phi] \quad (23)$$

in which  $H_\sigma = 35$  K,  $H_\pi = 6$  K, and [from the known values for crystalline YIG (Ref. 21)  $J = -33$  K at  $\phi = 126^\circ$ ] factor  $cH_\sigma \approx 1.6$ . Using the computer-generated  $\phi$  distribution in Eq. (23), we find a mean value  $\langle J \rangle = 28$  K appropriate for  $a$ -YIG.

Combining these mean exchange-parameter values  $\langle J \rangle$  with the mean exchange-field values  $\langle H_{ex} \rangle$  of Eq. (20), we find approximately the same ratio  $g\mu_B \langle H_{ex} \rangle / 2\langle J \rangle zS$  for all three speromagnets, namely  $0.06 \pm 0.01$ . The implication is that in the speromagnetically ordered phase near  $T=0$  the average NN spin is rotated by only about three to four degrees (i.e.,  $\sin^{-1}0.06$ ) towards antiparallel alignment from a random orientation.

In this sense the deviations of a speromagnetic spin alignment from a random orientational spin configuration seem small. However, within the above average, much larger counterbalancing rotations can possibly be present and there are strong indications that such is the case. The largest effect of these spin correlations is manifest in the exchange-field distribution for which (Fig. 7) no recognizable feature of a random-orientation spin distribution remains at all. In fact, the correlations reflect primarily a quasicontstraint on the  $z$  nearest-neighbor spin orientations, restricting their sum to small values.

In spite of this, for many other quantities involving spin orientations these same correlations may appear to be minor, only modestly perturbing the relevant distribution function from its random form. The hyperfine field is one such example (see Fig. 8). The formal manner in which the same set of variables can be "quasirandom" with respect to one distribution function but dramatically nonrandom with respect to another can be trivially demonstrated by use of Eq. (5). In this equation for the distribution of a function  $h = x_1 + x_2 + \dots + x_z$ , the re-

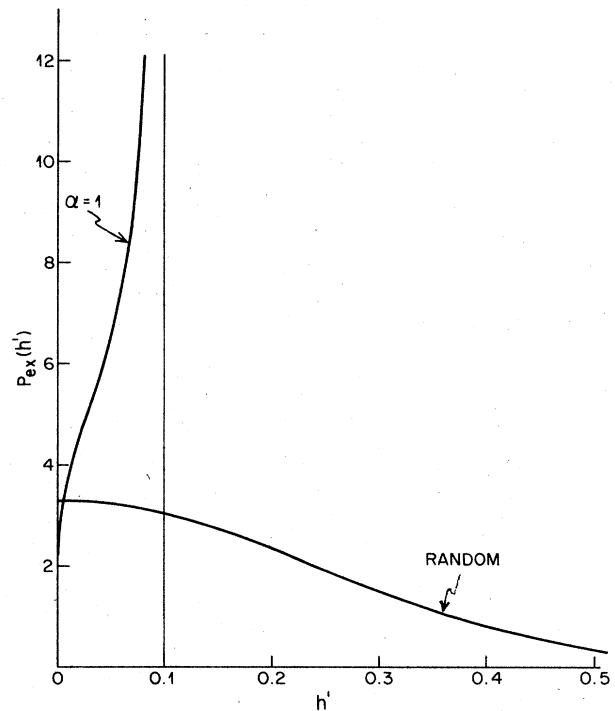


FIG. 7. Exchange distribution  $p_{ex}(h')$ , where  $h' = g\mu_B H_{ex} / 2JSz$ , as deduced from the Mössbauer data on amorphous speromagnets (drawn for  $\alpha=1$ ) is contrasted with the equivalent distribution for truly randomly oriented spins, viz.  $p_6(h/6)$  of Eq. (5).

striction of any single variable  $x_n$  from the random set  $x_1, \dots, x_z$  to the value  $x_n = 0$  perturbs  $p_z(h)$  to  $p_{z-1}(h)$ , a small effect if  $z \gg 1$ . On the other hand, with respect to the function  $h = x_1 x_2 \times \dots \times x_z$ , the same restriction collapses  $p_z(h)$  to a  $\delta$  function at  $h = 0$  for all  $z$ .

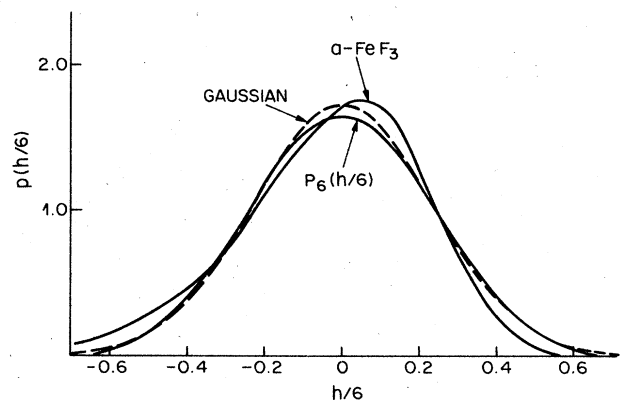


FIG. 8. Normalized probability distribution  $p_6(h/6)$  from Eq. (5) and Fig. 1 for a reduced projection  $h/6 = \frac{1}{6} \sum_{n=1}^6 \cos\theta_n$  of  $z=6$  randomly oriented spins is compared with a symmetric Gaussian of equal area and RMS linewidth (dashed curve) and with the scaled hyperfine distribution as measured for  $a$ -FeF<sub>3</sub> at 4.2 K (asymmetric solid curve).

## VII. SUMMARY

Hyperfine-field tails at low fields are observed consistently (by Mössbauer-Zeeman spectroscopy) in amorphous ferric speromagnets but not in amorphous ferromagnets. They indicate the existence of low-exchange-field sites in the distribution  $p_{\text{ex}}(H_{\text{ex}})$  of exchange fields  $H_{\text{ex}}$  in speromagnets caused by frustration. The shape of the hyperfine distribution spectrum at low temperatures reflects primarily the coordination and orientational distribution of NN spins via the supertransferred hyperfine component. Its detailed form, including the tails, can be used to deduce both the mean local magnetic coordination and the distribution  $p_{\text{ex}}(H_{\text{ex}})$  of exchange fields in actual speromagnets.

Using the 4.2-K Zeeman spectra for speromagnetic  $a$ -YIG,  $a$ -FeF<sub>3</sub>, and  $a$ -NaFeF<sub>4</sub>, we conclude that although these materials are structurally quite different in terms of local coordinations ( $a$ -YIG is quasirandom-packed; the others locally quasicrystalline) they are remarkably similar, though not identical, as regards the shape of  $p_{\text{ex}}(H_{\text{ex}})$ ; see Figs. 5 and 6. This distribution, however, is grossly

different from that corresponding to truly randomly-oriented spins (Fig. 7) and reflects an extremely large modulation of exchange distribution produced by the exchange-induced spin correlations. The implied correlation is one of quasicontstraint on the  $z$  nearest neighbors of any given spin, restricting their vector sum to small values.

This finding for NN-exchange ferric speromagnets contrasts with the equivalent situation in long-range exchange (i.e., RKKY) spin glasses for which computer simulations suggest that spin correlations only modestly perturb the analogous random-spin-orientational distribution. Although the *average* spin orientational perturbation from true randomness towards local antiparallel alignment (induced by the very dominantly antiferromagnetic NN exchange) is only between three and four degrees in each of the speromagnets  $a$ -YIG,  $a$ -FeF<sub>3</sub>, and  $a$ -NaFeF<sub>4</sub>, they are correlated in such a way as to produce a dramatic effect on the distribution function of the correlation-driving property itself (viz.  $H_{\text{ex}}$ ). Other distributions involving these same correlated spins [in particular, the hyperfine distribution of Fig. (8)] are only weakly perturbed from their random forms.

- 
- <sup>1</sup>J. M. D. Coey, J. Appl. Phys. **49**, 1646 (1978).  
<sup>2</sup>I. A. Campbell, S. Senoussi, F. Varret, J. Teillet, and A. Hamzic, Phys. Rev. Lett. **50**, 1615 (1983).  
<sup>3</sup>G. Ferey, Rev. Phys. Appl. **15**, 1043 (1980).  
<sup>4</sup>M. Eibschutz, M. E. Lines, L. G. Van Uitert, H. J. Guggenheim, and G. J. Zydzik, Phys. Rev. B **29**, 3843 (1984).  
<sup>5</sup>M. Eibschutz, M. E. Lines, H. J. Guggenheim, L. G. Van Uitert, and G. J. Zydzik, J. Phys. C (to be published).  
<sup>6</sup>M. Eibschutz, M. E. Lines, H. S. Chen, and T. Masumoto, J. Phys. F **14**, 505 (1984).  
<sup>7</sup>C. Held and M. W. Klein, Phys. Rev. Lett. **35**, 1783 (1975).  
<sup>8</sup>L. R. Walker and R. E. Walstedt, Phys. Rev. B **22**, 3816 (1980).  
<sup>9</sup>M. A. Ruderman and C. Kittel, Phys. Rev. **96**, 99 (1954); K. Yosida, *ibid.* **106**, 893 (1957); T. Kasuya, Progr. Theor. Phys. **16**, 45 (1956).  
<sup>10</sup>M. Eibschutz, M. E. Lines, and H. S. Chen, Phys. Rev. B **28**, 425 (1983).  
<sup>11</sup>M. Eibschutz and M. E. Lines, Phys. Rev. B **25**, 4256 (1982); **25**, 6042 (1982).  
<sup>12</sup>G. A. Sawatzky and F. Van der Woude, J. Phys. (Paris) Colloq. **35**, C6-47 (1974).  
<sup>13</sup>B. C. Tofield, J. Phys. (Paris) Colloq. **37**, C6-539 (1976).  
<sup>14</sup>M. E. Lines and M. Eibschutz, Phys. Rev. B **30**, 1416 (1984).  
<sup>15</sup>M. E. Lines, Phys. Rev. B **21**, 5793 (1980).  
<sup>16</sup>J. M. D. Coey and P. J. K. Murphy, J. Non-Cryst. Solids **50**, 125 (1982).  
<sup>17</sup>E. M. Gyorgy, K. Nassau, M. Eibschutz, J. V. Waszczak, C. A. Wang, and J. C. Shelton, J. Appl. Phys. **50**, 2883 (1979).  
<sup>18</sup>M. Henry, F. Varret, J. Teillet, G. Ferey, O. Massenet, and J. M. D. Coey, J. Phys. (Paris) Colloq. **41**, C1-279 (1980).  
<sup>19</sup>J. M. Dance, F. Menil, D. Hanzel, R. Sabatier, A. Tressaud, G. le Flem, and P. Hagenmuller, Physica **86-88B**, 699 (1977).  
<sup>20</sup>M. E. Lines, Phys. Rev. B **20**, 3729 (1979).  
<sup>21</sup>P. J. Wojtowicz, Phys. Lett. **11**, 18 (1964).